Wasit Journal of Engineering Sciences
Journal homepage: https://ejuow.uowasit.edu.iq
Vol. 13 No. 4 December 2025, pp.6-17
https://doi.org/10.31185/ejuow.v13i4.700

ISSN 2305-6932
Original Research

Spectral Efficiency of mmWave Massive MIMO Systems with Hybrid Beamforming

Sajjad Kadhim Mohammed[1], Hassan Fahad Khazaal[1], Hamed Al-Raweshidy[2], Ismail Sharhan Hburi[1], Ruwa Mohammed Hussein[1], Asmaa Kadhum Aliwy[1],

[1]Electrical Engineering Department, College of Engineering, Wasit University, Wasit, Iraq
[2]Electronic and Electrical Engineering, Brunel University of London, UK

Corresponding Author Email: sajjmoh@uowasit.edu.iq

Received May.7, 2025 Revised Jul.25, 2025 Accepted Jul.27, 2025 Online Dec.1, 2025

ABSTRACT

Millimeter wave communications (mmWave) has been considered a key enabling technique for 5G systems since it offers orders of magnitude more spectrum than current frequency bands. Unlike conventional multiple input multiple output (MIMO) networks, beamforming in millimeter-wave systems cannot be accomplished using digital techniques since only a limited number of analog-to-digital converters and mixers can be handled due to their cost and power consumption. Recently, there has been a lot of interest in a hybrid beamforming transceiver design, which includes an analog and digital beamformer, as a less expensive alternative. However, the optimal design for these hybrid beamformers has not yet been fully established. In order to approach the complex performance of the fully digital beamformer, this work will provide efficient alternative minimization techniques for a hybrid beamforming structure, namely the manifold-based geometric fully-connected antennas. According to simulation data on bandwidth efficiency, the proposed iterative algorithm performs much better than the baseline hybrid beamforming approach, namely the MMSE-MP algorithm (about 6.8% for a particular situation). Additionally, based on the recommended techniques, comparing the simulation results of the two hybrid beamforming structures will yield vital design information.

Keywords: Massive multiple-input multiple-output, Bandwidth Efficiency, Millimeter Waves, fully-connected Structure, hybrid beamforming, manifold geometric. massive multiple-input multiple-output, Bandwidth Efficiency.

1. Introduction

The capacity of wireless networks must increase significantly to meet the growing demands for high-data-rate multimedia access. In particular, the next generation of 5G networks aim to reach the predicted 1000X capacity increase by 2020 [1]. One way to boost the capacity is to use physical layer techniques such as massive multiple-input multiple-output (mMIMO) and sophisticated channel coding to increase the bandwidth efficiency [3], [4]. Area bandwidth efficiency may be further increased by network densification, which includes the deployment of micro Cells of Networks [4], the facilitation of device-to-device communications [5], [6], and improved cooperation, such as Cloud-Radio access networks [7], [8]. However, a major obstacle to further capacity increase is the spectrum scarcity of the present cellular networks. Therefore, it is essential to take advantage of unutilized spectrum bands, such as those that have not yet been used for cellular communications. Recently, millimeter wave (mm-Wave) bands have emerged as a top candidate for extra spectrum in 5G cellular networks, with a theoretical bandwidth of 10 GHz. This notion is supported by recent experiments that demonstrated the feasibility of mmWave outdoor cellular communications [9], [12]. Once, the main obstacles to the feasibility of mmWave cellular networks were the massive route rain and loss attenuation caused by the tenfold increase in carrier frequency [11]. Due to the short wavelength of millimeter-wave transmissions, mmWave MIMO

beamforming may utilize large-scale antennas at transceivers to produce highly directed beams and provide significant beamforming advantages to compensate for route loss. Moreover, sending numerous data streams via spatial multiplexing can increase spectral efficiency even more. Conventional MIMO systems often employ digital beamformers at baseband for beamforming, which can change the phase and amplitude of the signals. However, completely digital beamforming requires radio frequency chains, which contain signal mixers and analog-to-digital converters. The number of these chains equals the number of antenna components. Digital beamformers at baseband are frequently used in conventional MIMO systems for beamforming, which can alter the signals' amplitude and phase. However, radio frequency chains—which include signal mixers and analog-to-digital converters—are necessary for fully digital beamforming. The number of antenna components is equal to the number of these chains. Although the small wavelengths of mmWave carriers allow for the use of a large number of antennas, the high cost and power consumption of radio frequency chains prevent digital beamforming. The specific limits in mmWave MIMO systems have lately attracted a lot of attention to a hybrid beamforming design, which requires just a few chains of RF to interface between a low-dimensional baseband beamformer and a high-dimensional analog beamformer [13]. Because of their large dimensions, analog beamformers cannot be used in radio frequency stages with high power amplifiers [12]. A rule of thumb is produced by this heuristic, which is the implementation of analog beamformers using low-cost phase-shift circuits at the expense of losing the capacity to change the levels of the RF signals. These hybrid beamforming transceiver topologies may be classified as (totally and partially) linked schemes according to the mapping of antennas/RF-chains, which determines how many phase-shifters have to be used. The fully-connected antennas gain from the entire boost of beamforming for each radio frequency chain when antennas and RF chains are linked normally, that is, when one RF chain is coupled to one antenna. However, the partially-topology significantly reduces the hardware implementation complexity at the price of some beamforming gain by connecting each RF chain with only a section of the array. According to [13], the bandwidth efficiency of mmWave systems may be approximately maximized by lowering the Euclidean difference between hybrid beamformers and complete baseband beamformers. Phase shifters impose unit modulus limits, making the hybrid beamformer design a matrix factorization problem. The optimum method for creating hybrid beamformers is still unclear because of the unique unit modulus constraints, despite the fact that a lot of research has recently been done to tackle various matrix factorization difficulties [14], [15]. Existing works occasionally place extra limitations on analog beamformers in order to simplify the design of the analog section with unit modulus limits, which can lead to a decrease in efficacy. This motivates academics to use analog beamformers with unit modulus limitations to rethink beamformer design, most especially the matrix-factorization process. In particular, a better solution to the unit modulus limitation requires more thorough investigation. With alternative minimization as the main design approach, we will provide a variety of hybrid beamforming techniques in this study that will perform close to the best fully baseband beamformer. To find effective hybrid beamforming techniques for both linked partly and fully-connected antenna arrays, three novel algorithms based on the alternating minimization principle will be proposed.

1.1 Related Works

Hybrid beamforming is a new development for mmWave MIMO systems [16],[20]. The majority of the research is now focused on fully-connected assemblies [13], [21]. The most prevalent method, orthogonal matching pursuit (OMP_BF), consistently delivers respectable performance. For this technique, the columns of the passband beamforming vectors must be identified using vectors such as discrete Fourier transform beamformers [23], [24] and the channel's array response vectors [13], [21], [22]. The orthogonal matching pursuit hybrid beamformer problem may be seen as a matrix reconstruction with sparse constraints. Even while this greatly simplifies the design issue, performance loss is unavoidable when the spectrum of feasible analog beamforming approaches is limited. Hybrid beamforming is a novel concept in mmWave MIMO systems [16], [20]. The majority of current research focuses on completely linked assemblies [13], [21]. The most popular approach, orthogonal matching pursuit (OMP_BF), regularly produces acceptable results. To use this approach, the columns of the passband beamforming vectors must be identified using vectors like discrete Fourier transform beamformers [23], [24] and the channel's array response vectors [13], [21], [22]. The orthogonal matching pursuit hybrid beamformer issue may be represented as a matrix reconstruction with sparse constraints. Even while this considerably simplifies the design problem, performance loss is unavoidable when the number of viable analog beamforming options is restricted. Furthermore, there will be additional cost associated with obtaining the array response vector information ahead of time. More recent research has primarily focused on lowering the computing cost of the OMP method, such as recovering the output of matrix inversion in each

algorithm loop [21]. Unlike our prior work in [5], which was based on an algorithm, orthogonal matching pursuit, and the MMSE method, this paper addresses the Riemannian Manifold algorithm. Also, unlike the work in [22], which considers a random phase for the first analog beamforming, this study proposes a starting angle that accelerates the process.

1.2 Contributions

The hybrid beamformer problem in MIMO schemes (mmWave) is investigated in this paper. Our major design approach will be alternating minimization, which helps break the beamformer problem into two subtasks: the passband and baseband beamformer tasks. The provided methods will optimize the digital and analog beamformers sequentially. Below is an overview of our significant contributions:

• Develop an Alternating minimization approach based on manifold geometry to tackle hybrid beamformer tasks with unit modulus constraints.

• According to simulation data, the method outperforms the present approach while maintaining a fair processing complexity, and the algorithm effectively finds a near-optimal solution. Comprehensive comparisons are offered utilizing the specified approaches for revealing valuable design information. As a result, our findings unambiguously illustrate the effectiveness of the alternating technique as a critical strategy in mm-wave hybrid beamformer designs.

Table 1. Compiling a Summary of Symbols and Parameters.

Symbols	Definition	Symbols	Definition
$\mathbf{W}_{\mathrm{PB}}$	Tx Analog Beamforming	$\mathbf{H}$	Channel Matrix
$\mathbf{W}_{\mathrm{BB}}$	Tx Digital Beamforming	$\mathbf{g}_{\mathrm{t}}$	The Transmission Antennas' Response
M_{at}	The Transmission Antennas' Number	$\mathbf{g}_{\mathrm{r}}$	The Reception Antennas' Response
M_{ar}	The Reception Antennas' Number	M_{RF}	RF-Chain Number
$\mathbf{I}_{\mathrm{M}_{\mathrm{st}}}$	Identity Matrix	M_{st}	Data Stream Number
$\mathbf{Q}_{\mathrm{BB}}$	Rx Analog Beamforming	M_{C}	A Manifold Topological Space
$\mathbf{Q}_{\mathrm{PB}}$	Rx Digital Beamforming	$\mathbf{T}_{\mathrm{W}}\ \mathrm{M}_{\mathrm{C}}$	The Tangent Space at the Point (W)

2. Model of the System and Problem Formulation

The transmitter's output message may be expressed as,

$$\boldsymbol{m} = \boldsymbol{W_{PB}}\,\boldsymbol{W_{BB}}\ \boldsymbol{x} \ \ldots\ (\mathbf{1})$$

where, $\boldsymbol{W_{PB}} \in (\boldsymbol{M_{RF}} \times \boldsymbol{M_{st}})$ $\boldsymbol{and}$ $\boldsymbol{W_{BB}} \in (\boldsymbol{M_{at}} \times \boldsymbol{M_{st}})$, are the analog beamforming and digital beamforming, respectively, that are power-constrained by the squared norm (Frobenius).

$$\|\boldsymbol{W_{PB}}\,\boldsymbol{W_{BB}}\|_{\boldsymbol{F}}^{\boldsymbol{2}} = \boldsymbol{M_{st}} \ \ldots.\ (\mathbf{2})$$

Additionally, the symbol that has to be transmitted via M_st data streams while adhering to the following limitation is $x \in C\text{^}(M\_st \times 1)$ [18].

$$\Xi\{xx^{H}\} = \Xi\{|x|^{2}\} = \frac{1}{M_{St}}\ I_{M_{st}} \ \ldots (3)$$

Consequently, after the decoding process, the received stream will seem as follows:

$$y = P_t^{1/2}\ \ \boldsymbol{Q_{BB}^{H}}\boldsymbol{Q_{PB}^{H}}\ \boldsymbol{H}\ \boldsymbol{W_{PB}}\boldsymbol{W_{BB}}\ x + \ \boldsymbol{Q_{BB}^{H}}\boldsymbol{Q_{PB}^{H}}\, n \ \ldots.\ (4)$$

where the base-band combine beamformer is $Q\_BB \in (M\_RR \times M\_st)$, the pass-band combine beamformer is $Q\_PB \in (M\_ar \times M\_RR)$, the number of antennas at the receiver is M_ar, the transmission power is P_t, and the number of RF-chains at the combiner is M_RR. The scheme's bandwidth efficacy may therefore be represented using Shannon's formula as follows:

$$\eta_{SE} = ln\left(\left|I_{M_{st}} + \frac{P_t}{\sigma_n^2\, M_{st}}\ \boldsymbol{H}\ \boldsymbol{W_{BB}}\,\boldsymbol{W_{PB}}\ \ \boldsymbol{W_{PB}^{H}}\,\boldsymbol{W_{BB}^{H}}\ \boldsymbol{H^{H}}\right|\right) \quad \ldots (5)\ \text{(in nats/sec/Hz)}$$

where the operator | · | indicates the matrix's determinant and (·)^{H} indicates the matrix's conjugated transposition.

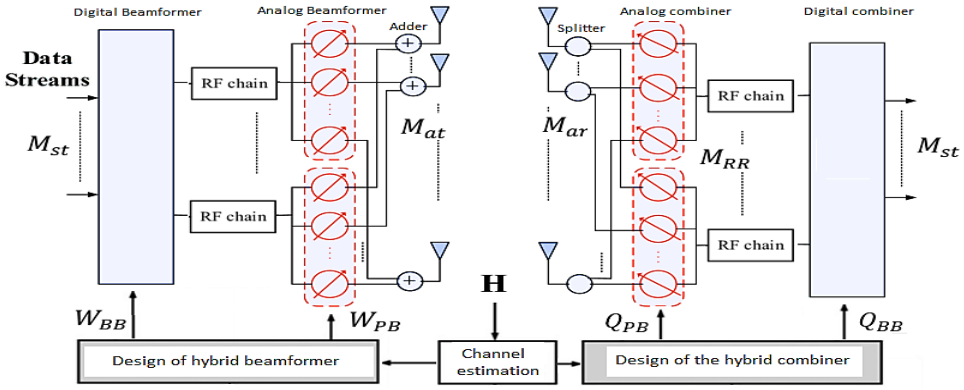

Figure 1. Structure of the Proposed Hybrid Beamforming System. From the Perspective of Spectrum Efficiency, the Fully-Connected BF Performs Better than the Sub-Connected Design Since it Provides a Greater RF Design-DoF.

2.1 Mm-Wave Channel's Model

The Saleh Valenzuela clustered channel model, a sparse model with few paths and scatters, has been generally accepted to describe the mmWave channel [19]. Without sacrificing generality, we assume that our array is square planar, with M_ar and M_at antennas on the transmission and reception edges, respectively. The channel's matrix $H \in C\hat{}(M\_ar \times M\_at)$ in Eq.(4) may be expressed as [18] by using the symbol L to indicate the number of routes in the channel that correspond to the number of scatters.

$$H = \left(\frac{M_{ar}\,.M_{at}}{M_{path}\,M_{cluster}}\right)^{\frac{1}{2}} \times \sum_{i=1}^{M_{cluster}} \sum_{j=1}^{M_{path}} \xi_{ij}.\, g_r(\theta_{ij})\;\; g_t(\phi_{ij})^{H} \qquad \dots(6)$$

The cluster or group number is M_cluster, the number of rays or routes in each group is M_path, the gain for the ith scatters' group within the jth path (complex-gaussian-distr.) is indicated by ξ_ij∈ ℂN(0,σ_ij^2), and ∑_(i∈ M_cluster)The vectors g_t (ϕ_ij) represent the transmitting antennas' response at ϕ_ij AoD (azimuth departure angle), and g_r (θ_ij) represent the reception antennas' response at θ_ij AoA (azimuth arrival angle). ▒σ_ij^2 indicates the normalizing factor that verifies that the mean of H_(F)^2 for the model is equivalent to M_ar M_at. Figure 2 illustrates the square planar uniform antenna of (N×N) antennas, whose response may be written as follows:

$$g(\theta_{ij},\phi_{ij}) = \frac{\left[1,\dots,exp\left(\frac{2\pi L}{\lambda}\left[p.\cos\phi_{ij} + q.\sin\theta_{ij}.\;\sin\phi_{ij}\right]\right)\right]^{T}}{N}, \qquad for\ all\ \ p,q\ \in\{0,1,\dots N\} \qquad \dots(7)$$

Here, λ is the wavelength of the signal and L is the distance between the elements in the array.

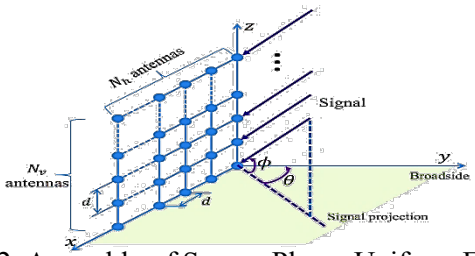

Figure 2. Assembly of Square Planar Uniform Elements.

2.2 System efficiency formula

The development of analog and digital beamforming, or $\boldsymbol{W}_{PB}$, $\boldsymbol{W}_{BB}$, is our main emphasis in this work. For maximum bandwidth efficiency, they can be presented as follows:

$$\textbf{Problem:} \quad \max_{W_{PB},W_{BB}} f_1(\boldsymbol{W_{PB}},\boldsymbol{W_{BB}})$$

$$\boldsymbol{C^1}: \ \boldsymbol{W_{PB}}(i,j) \in \omega \quad \forall i,j$$
$$\boldsymbol{C^2}: \ \|\boldsymbol{W_{PB}}\boldsymbol{W_{BB}}\|_F^2 \ = M_{st} \qquad \ldots(8)$$

Where, $f_1(\ \boldsymbol{W_{PB}}, \boldsymbol{W_{BB}}) = \ ln\left(\left|I_{M_{st}} + \frac{P_t}{\sigma_n^2 N_{st}} H \ W_{BB} \ W_{PB} \quad W_{PB}^H \ W_{BB}^H \ H^H\right|\right)$, For an infinite-resolution phase shift network, the realistic set of analog beamformers is represented by V, which is equivalent to the unit-modulus requirement, $\left|(\boldsymbol{W}_{PB})_{ij}\right| \ = 1$.

2.2.1 Baseband Digital Beamforming

Alternating Minimization is a popular and empirically successful approach to the problems associated with the optimization of different variable subsets. Accordingly, the digital beamforming matrix W_BB for maximum bandwidth efficiency in Eq. (8) can be expressed as follows,

$$\boldsymbol{W_{BB}} = \ (\boldsymbol{W_{PB}}^{\boldsymbol{T}}\boldsymbol{W_{PB}})^{-1} \ \boldsymbol{W_{PB}}^{\boldsymbol{T}} \ \boldsymbol{W_{opt}} = \ \boldsymbol{W_{PB}}^{\dagger} \ \boldsymbol{W_{opt}} \qquad \ldots(9)$$

Refer to Eq.(A-1) through Eq.(A-3) in Appendix A for a complete proof.

2.2.2 Passband Analog Beamforming (Riemannian-manifold)

Since each antenna in the fully-connected array is linked to every RF chain in the suggested topology, figure 1, the feasible values of the passband beamformer might be determined by $\left|(\boldsymbol{W}_{PB})_{ij}\right| = 1$. In the next alternating phase, we solve $\boldsymbol{W}_{BB}$ and search for an analog beamformer that achieve minimum distance $f_4(\boldsymbol{W}_{PB}, \boldsymbol{W}_{BB}) = \left\|\boldsymbol{W}_{opt} - \ \boldsymbol{W}_{PB}\boldsymbol{W}_{BB}\right\|_F^2$ over the variable matrix $\boldsymbol{W}_{PB}$. The main obstacles are the unit modulus limits, which are essentially nonconvex. To the best of the authors' knowledge, there is no one-size-fits-all approach to solving Eq (8). In the following, we will introduce an effective manifold optimization method to find a near-optimal solution to the equation. As shown in figure 3, a manifold topological M is a space that is comparable to a Euclidean space at each point. In other words, any point's neighbourhood inside a manifold is homeomorphic to Euclidean space. Additionally, the tangential space $\mathbf{T}_{\mathrm{W}}\ M$ is made up of the tangent vectors η of the curves across a certain point (w) on the manifold. Most applications involve manifolds that fall into a certain category of topological manifolds called Riemannian manifolds. The Riemannian metric, an inner linear product given on the tangential space $\mathbf{T}_{\mathrm{W}}\ \mathrm{M}_C$ that exists on a Riemannian manifold M, is used to measure angles and distances on manifolds. In particular, one can apply Riemannian geometric calculus to a Riemannian manifold. The rich metric of the Riemannian manifold allows for the definition of gradients of cost functions. Moreover, optimization on a Riemannian manifold is locally equivalent to smooth constrained optimization on a Euclidean space. Consequently, a conjugate-gradient method in Euclidean space can determine their equivalent on the specified Riemannian manifolds. In the following, we will provide a quick overview of this equivalency. Manifolds that belong to a certain class of topological manifolds known as Riemannian manifolds are used in the majority of applications. Angles and distances on manifolds are measured using the Riemannian metric, which is an inner linear product provided on the tangential space $\mathbf{T}_{\mathrm{W}}\ \mathrm{M}_C$. Specifically, a Riemannian manifold can be treated as a Riemannian geometric calculus. Gradients of cost functions may be defined thanks to the Riemannian manifold's rich metric. Furthermore, smooth constrained optimization on a Euclidean space is locally identical to optimization on a Riemannian manifold. Their equivalent on the given Riemannian manifolds may thus be found using a conjugate-gradient approach in Euclidean space. A brief synopsis of this equivalence will be given below. The tangent vectors define the directions in which a particular point x on the manifold M_C can move and the tangent space at (w) can then be denoted as $\mathbf{T}_{\mathrm{W}}$ M. Observe that a complex circle manifold $\mathrm{M}_{CC}{}^{m}$, where $m = \ M_t \ M_{RF}$, is formed by the vector $\boldsymbol{w}$ = vec ($\mathbf{W_{PB}}$). The searching range of optimizing task in Eq. (8) is consequently over a product of m circles within the Riemannian sub-manifold (complex plane). In mm-wave MIMO systems, the shape depicted in figure1 is commonly used. It makes the beamformer design problems impervious by this elementwise constraint by preventing any entry from obtaining unit modulus in the analog beamforming matrix. In order to solve equation (8), this research will specifically examine an Alternating Minimization technique based on manifold optimization principles by showing that a Riemannian manifold may be created when there are limitations on the unit modulus. The Riemannian-gradient vector in this situation is provided as follows:

$$grad\ f_4(\boldsymbol{W_{PB}}) = \nabla f_4(\ \boldsymbol{W_{PB}}) - Rel.(\nabla f_4(\ \boldsymbol{W_{PB}}).\ \ \boldsymbol{W_{PB}}^{*}).\ \boldsymbol{W_{PB}} \quad \ldots.(10)$$

where the elementwise product is indicated by the operation (.). Refer to Eq.(B-1) through Eq.(B-6) in Appendix B for a complete proof.

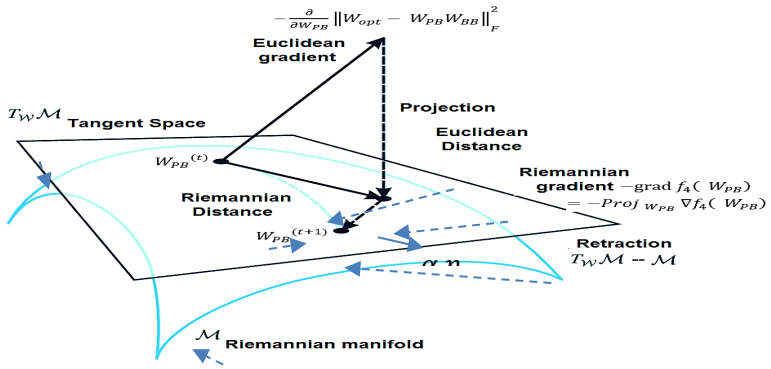

Figure 3. A Riemannian Manifold Tangent Space and Tangent Vector.

Complexity Analysis

The convergence of the objective function for the proposed Beamforming algorithm can be ensured via the upper bound constraints. The computational complexity for this process is mainly characterized by the number of iterations of the proposed Algorithm indicated by the blue dotted line in the Flowchart of figure 4. The complexity analysis includes computations of the Riemannian-gradient vector with complexities of, $\boldsymbol{\mathcal{O}}\left(\boldsymbol{M_{at}M_{RF}}^{\boldsymbol{2}} + \boldsymbol{M_{at}M_{RF}M_{st}}\right)$. Consequently, the complexity of the optimization is, $\boldsymbol{\mathcal{O}}\left(t.\left[\boldsymbol{M_{at}M_{RF}}^{\boldsymbol{2}} + \boldsymbol{M_{at}M_{RF}M_{st}}\right]\right)$, given that (t) is the over-all algorithm iteration numbers.

Table 2. The Pseudo-Code for the Proposed Optimization Algorithm-I

Start the algorithm:

Set the system's initial circumstances, such as the channel matrix H, the iteration index: t = 0, last iteration N, the optimal beamforming $\boldsymbol{W_{opt}} = \boldsymbol{W_1}$, and the total transmit power P_t.

1st STAGE; Initial beamforming:

1. Determine the corresponding initialize digital beamforming $\boldsymbol{W_{opt}}$.
2. Set the initial phases of the Analog beamforming,

$$\measuredangle\left\{\boldsymbol{W_{PB}}^{(0)}\right\} = \measuredangle\left\{\boldsymbol{W_{opt}}.\boldsymbol{W_{BB}}^{(0)^{H}}\right\}$$

3. To guarantee the power constraint, scale the result: $\boldsymbol{W_{BB}^{(0)}} = \boldsymbol{W_{BB}^{(0)}}.\frac{\sqrt{\boldsymbol{M_{St}}}}{\boldsymbol{W_{PB}^{(0)}W_{BB}^{(0)}}}$

2nd STAGE; Iterative Sub-optimal approach;

1. Determine the Euclidean gradient w.r.t $\boldsymbol{W_{PB}}$,

$$\boldsymbol{\nabla f_4(W_{PB}, W_{BB})|_{V_{PB}}} = \frac{\boldsymbol{\partial}}{\boldsymbol{\partial W_{PB}}}\left\|\boldsymbol{W_{opt}} - \boldsymbol{W_{PB}W_{BB}}\right\|_{\boldsymbol{F}}^{\boldsymbol{2}} = \mathbf{vect}\left(-\mathbf{2}\left(\boldsymbol{W_{opt}} - \boldsymbol{W_{PB}W_{BB}}\right)\boldsymbol{W_{BB}}^{\boldsymbol{H}}\right.$$

2. Determine the gradient in Riemannian metric $\boldsymbol{\eta^{(t)}}$ as the projection of $\boldsymbol{\nabla f_4}$ onto the tangent space; $\boldsymbol{grad\, f_4(W_{PB})} = \boldsymbol{\nabla f_4(W_{PB})} - \boldsymbol{Rel.}\left(\boldsymbol{\nabla f_4(W_{PB})}.\ \boldsymbol{W_{PB}}^{*}\right).\boldsymbol{W_{PB}}$
3. Determine the tangent vector $\boldsymbol{\alpha\,\eta^{(t)}}$ retraction at the current position $\boldsymbol{v^{(t)}}$;

$$\boldsymbol{w^{(t+1)}} = \boldsymbol{Ret_v}\left(\boldsymbol{\alpha\,\eta^{(t)}}\right) = \boldsymbol{vect}\left[\frac{\left(\boldsymbol{w^{(t)}} + \boldsymbol{\alpha\,\eta^{(t)}}\right)_{\boldsymbol{i}}}{\left|\left(\boldsymbol{w^{(t)}} + \boldsymbol{\alpha\,\eta^{(t)}}\right)_{\boldsymbol{i}}\right|}\right]$$

Update the digital beamforming;

$$\boldsymbol{W_{BB}^{(t+1)}} = (\sigma_n^2 \boldsymbol{I_{A_{st}}} + \boldsymbol{W_{PB}}^{(t)^T} \boldsymbol{W_{PB}}^{(t)})^{-1} \boldsymbol{W_{PB}}^{(t)^T} \boldsymbol{W_{opt}}$$

1. Checking the end of iterations:

If t = $\boldsymbol{N}$, Then; go to step (8).

Else: Update the counter (t =t +1), and go to step (4) (next iteration).

End If

End Return Digital and Analog Beamforming, $\boldsymbol{W_{BB}}$, $\boldsymbol{W_{PB}}$.

3. Numerical Analysis

In this part, we assess the performance of the suggested hybrid beamformer algorithm by numerical simulation. As baseline algorithms or criteria for comparison, we employ the iterative algorithm for sub-connected architecture (MMSE-MP), which considers techniques like the traditional optimal full digital scheme, Opt. beamforming [24], the sparse approximation (Matching Pursuit algorithm) for the passband beamforming, and the least mean squared error beamforming (MMSE) technique for the baseband beamforming [7].

All benchmarks are considered with the same configuration, also all investigations are conducted in a MATLAB environment (version R2019b) run on a Processor of Intel (TM) Core i5 @ 2.40 GHz, 64-bit operating system. Table 2 shows the system parameters that have been configured in the simulation. It is worth noting that the motives for deciding on these specific simulation scenarios are to meet the requirements and conditions of 5G mmWave communication systems, e.g., the propagation setting and channel conditions are according to the model employed in reference [22] and the parameters suggested in reference [7] for the aforementioned system (see Table 2).

Table 3. System Parameters Employed in the Simulation.

Parameter	Setting
Number of channel realization	10^4
User antenna's number	M_{ar} =32 elements
Number of RF-chain	$M_{RF} = [5; 20]$
Base station antenna's number	$M_{at} = (128, 256)$ elements
Number of Data-Stream	$M_{st} = \{2, 4, 6\}$
Transmit power rang	$P_t = [-10; 15]$ dB
The propagation setting	
Number of the clusters	$M_{cluster} = 6$
The azimuths' spread angles	10 (Uniform distribution degrees)
Number of the paths	$M_{path} = 10$ rays
Variance of channel path (Gaussian distribution)	$\sigma_{ij}^2 = 1$,
Array structure	Squared planner sub-connected array
The passband-BF initial angle	according to equation (11)

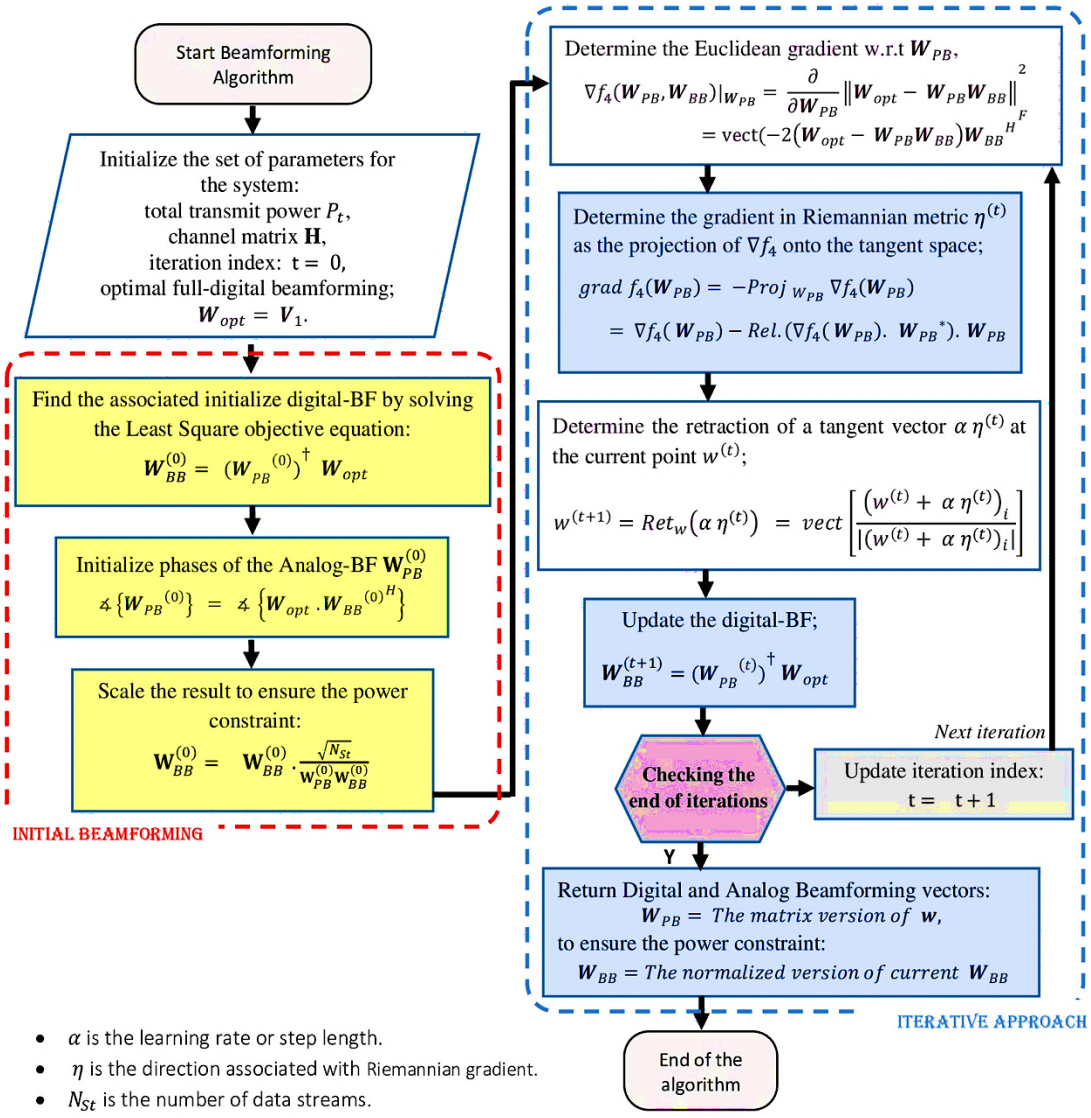

Figure 4. Flowchart of the Proposed Beamforming Algorithm.

4. Results and Discussion (Assessment of Bandwidth Efficiency)

This section investigates the bandwidth efficiency that can be achieved by different approaches where the number of RF in the chains is equal to the number of information streams. Since fewer RF links are not possible, this is the worst-case situation. First, Figure 5 shows the throughput of a 128 x 64 mm-Wave scheme for various beamform algorithms as the transmitted power increases, where the number of information streams ($M_{sr} = 4$) on the channel is equal to the number of RF-chains in the scheme. This figure shows that, particularly at high power-region, the proposed hybrid-beamforming technique allows for a significant improvement in bandwidth efficiency over the MMSE-MP baseline scheme (the system's bandwidth efficiency is roughly 6.8% higher than the standard Matching Pursuit algorithm technique at power of 10 dB). Opt-digital-BF, the full-digital system, performs better than our method in terms of bandwidth efficiency, but at the cost of much higher power consumption and hardware complexity. Figure 7 compares the bandwidth performance of the proposed method with the matching pursuit sparse approximation technique (MMSE-MP) versus the number of RF-chains employed. As the number of RF-chains increases, the bandwidth efficiency will increase logarithmically rather than linearly, as the picture illustrates. The number of phase-shifters and the number of RF-chains in the proposed architecture do not directly correspond. figure 7 displays how the number of transmitting antennas employed affects the bandwidth performance of the proposed strategy. The effects of the number of RF chains are then investigated. Assuming six data streams are sent, figure 8 compares different methods. As expected, as

the number of transmitting antennas rises, the spectral performance will improve due to the increased degree of freedom of the MIMO system. Figure 9 illustrations that the gap, in terms of the time complexity performance, between the matching pursuit sparse approximation scheme (MMSE-MP) and the proposed scheme become narrower with the growing of the RF-gain number.

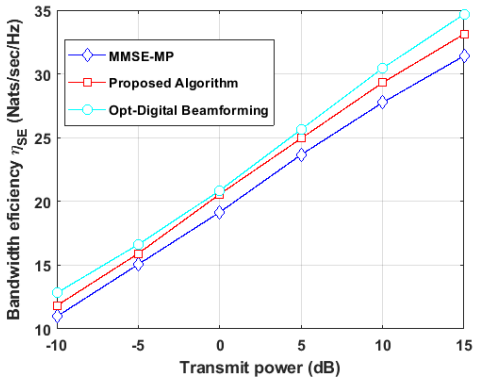

Figure 5. The Bandwidth Performance Versus Transmitted Power, $M_{cluster} = 6$.

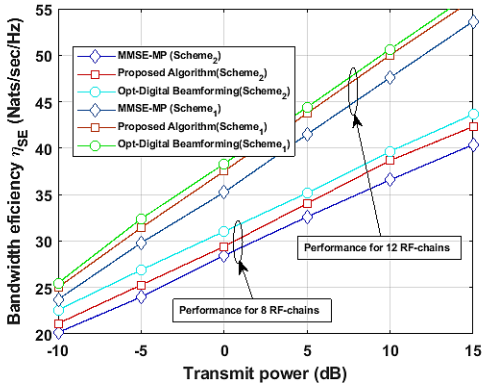

Figure 6. The Bandwidth Performance Versus Transmitted Power for Different RF-Chain and $M_{at} = (128)$ Elements.

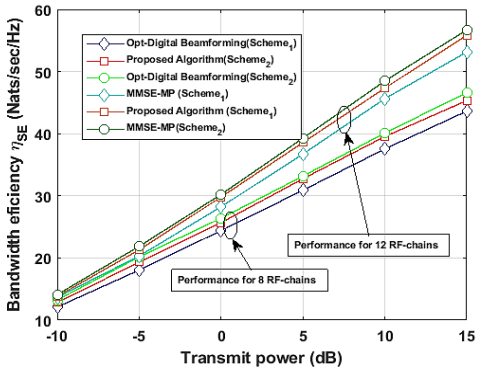

Figure 7. The Bandwidth Performance Versus Transmitted Power, $M_{cluster} = 6$. for Different RF-Chain and $M_{at} = (256)$ Elements.

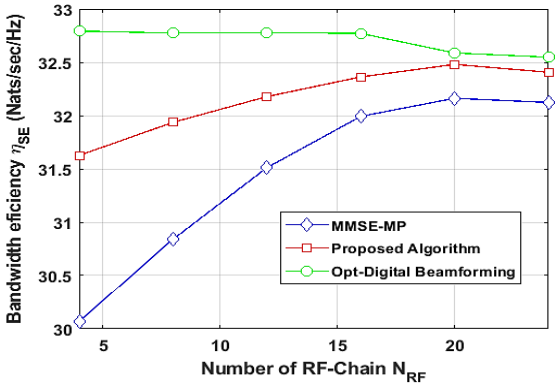

Figure 8. The Bandwidth Performance Versus Number of RF-Chains, $M_{cluster} = 6$.

5. Conclusions

Based on the alternating minimization principle, we proposed a straightforward design technique for hybrid beamforming in fully-connected mmWave MIMO systems in this paper. The following useful design information was obtained from the simulations' results:

- In a fully-connected topology, hybrid beamformers can function similarly to completely digital beamformers when the number of RF chains is somewhat more than the number of information streams. Given the growing cost and power consumption, further RF chains are not necessary. In addition, it makes financial sense to implement a sizable number of RF chains in order to maximize bandwidth efficiency.
- In Addition, our results have clearly demonstrated the effectiveness of alternating minimization in designing hybrid beamformers for mmWave MIMO systems. Furthermore, additional investigation is required to conduct a more comprehensive convergence analysis and optimality characterization of the proposed approach.
- Finally, as a future work trend, the work can be extended to partially connected architectures and analyzing the robustness of the scheme under channel estimation errors to handle rapidly changing channel conditions.

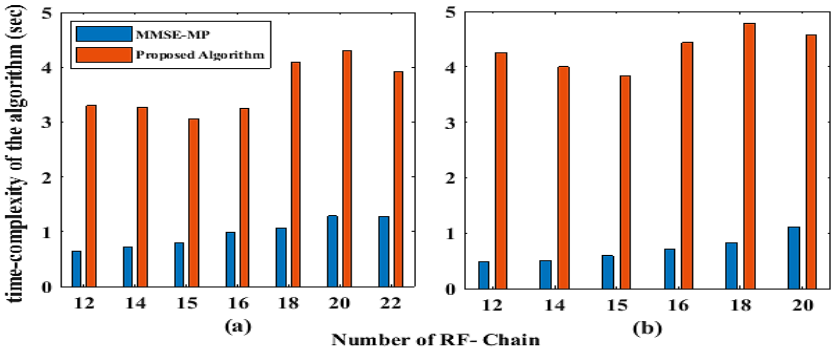

Figure 9. The Time Complexity Performance Versus Number of the RF-Chain:

(a) $M_{at} = (128)$ Elements. (b) $M_{at} = (256)$ Elements.

Author Contributions

All authors proposed the research problem. Sajjad K. incorporated the use of mm-wave within the fully-connected structure. Hassan F. Khazal formulated the mathematical model, Hamed Al-Ruwaishidi supervised the software model using MATLAB commands to express the mathematical equations. Ismail H. developed a suitable model for the wireless channel, which is the Saleh Valenzuela model. Roaa M. revised and wrote the theoretical part of the research. Asmaa A. obtained the theoretical results of the research to compare them with some approved models for the mm-wave system.

References

[1] J. G. Andrews *et al.*, "What will 5G be?," *IEEE J. Sel. areas Commun.*, vol. 32, no. 6, pp. 1065–1082, 2014.

[2] H. Fahad and I. Hburi, "ConvNet-based multi-antenna precoder design for green communication," in *Proceedings of Sixth International Congress on Information and Communication Technology: ICICT 2021, London, Volume 4*, Springer, 2021, pp. 357–365.

[3] J. Hoydis, S. Ten Brink, and M. Debbah, "Massive MIMO in the UL/DL of cellular networks: How many antennas do we need?," *IEEE J. Sel. Areas Commun.*, vol. 31, no. 2, pp. 160–171, 2013.

[4] C. Li, J. Zhang, and K. B. Letaief, "Throughput and energy efficiency analysis of small cell networks with multi-antenna base stations," *IEEE Trans. Wirel. Commun.*, vol. 13, no. 5, pp. 2505–2517, 2014.

[5] I. Hburi and H. F. Khazaal, "A Neural Network Approach for Spectral and Energy Efficient Multiple Antenna Systems," in *2021 1st Babylon International Conference on Information Technology and Science (BICITS)*, IEEE, 2021, pp. 154–159.

[6] G. Bartoli *et al.*, "Beamforming for small cell deployment in LTE-advanced and beyond," *IEEE Wirel. Commun.*, vol. 21, no. 2, pp. 50–56, 2014.

[7] N. Qasim, I. Hburi, and H. S. Al Ammar, "Intelligent Reconfigurable surface technique for Multiple Antenna Communication System," *Wasit J. Eng. Sci.*, vol. 12, no. 3, pp. 15–24, 2024.

[8] Y. Shi, J. Zhang, K. B. Letaief, B. Bai, and W. Chen, "Large-scale convex optimization for ultra-dense cloud-RAN," *IEEE Wirel. Commun.*, vol. 22, no. 3, pp. 84–91, 2015.

[9] Y. Shi, J. Zhang, and K. B. Letaief, "Group sparse beamforming for green cloud-RAN," *IEEE Trans. Wirel. Commun.*, vol. 13, no. 5, pp. 2809–2823, 2014.

[10] I. Hburi, A. Assad, and H. Fahad, "A Deep Neural Network Approach to Max-Min Fair Precoder for Multiple Antenna Systems," in *2022 3rd Information Technology To Enhance e-learning and Other Application (IT-ELA)*, IEEE, 2022, pp. 123–128.

[11] S. Hur, T. Kim, D. J. Love, J. V Krogmeier, T. A. Thomas, and A. Ghosh, "Millimeter wave

beamforming for wireless backhaul and access in small cell networks," *IEEE Trans. Commun.*, vol. 61, no. 10, pp. 4391–4403, 2013.

[12] E. Torkildson, U. Madhow, and M. Rodwell, "Indoor millimeter wave MIMO: Feasibility and performance," *IEEE Trans. Wirel. Commun.*, vol. 10, no. 12, pp. 4150–4160, 2011.

[13] T. S. Rappaport, R. W. Heath Jr, R. C. Daniels, and J. N. Murdock, *Millimeter wave wireless communications*. Pearson Education, 2015.

[14] M. R. Akdeniz *et al.*, "Millimeter wave channel modeling and cellular capacity evaluation," *IEEE J. Sel. areas Commun.*, vol. 32, no. 6, pp. 1164–1179, 2014.

[15] O. El Ayach, S. Rajagopal, S. Abu-Surra, Z. Pi, and R. W. Heath, "Spatially sparse precoding in millimeter wave MIMO systems," *IEEE Trans. Wirel. Commun.*, vol. 13, no. 3, pp. 1499–1513, 2014.

[16] P. Jain, P. Netrapalli, and S. Sanghavi, "Low-rank matrix completion using alternating minimization," in *Proceedings of the forty-fifth annual ACM symposium on Theory of computing*, 2013, pp. 665–674.

[17] M. Cai, "Modeling and mitigating beam squint in millimeter wave wireless communication," 2018, *University Of Notre Dame*.

[18] A. A. Majeed, D. Ali Saed, and I. Hburi, "AI-Based Q-Learning Approach for Performance Optimization in MIMO-NOMA Wireless Communication Systems," *Int. J. Electr. Comput. Eng. Syst.*, vol. 14, no. 8, pp. 843–851, 2023.

[19] P. Drineas and M. W. Mahoney, "Approximating a gram matrix for improved kernel-based learning," in *International Conference on Computational Learning Theory*, Springer, 2005, pp. 323–337.

[20] W. Roh *et al.*, "Millimeter-wave beamforming as an enabling technology for 5G cellular communications: Theoretical feasibility and prototype results," *IEEE Commun. Mag.*, vol. 52, no. 2, pp. 106–113, 2014.

[21] S. Sun, T. S. Rappaport, R. W. Heath, A. Nix, and S. Rangan, "MIMO for millimeter-wave wireless communications: Beamforming, spatial multiplexing, or both?," *IEEE Commun. Mag.*, vol. 52, no. 12, pp. 110–121, 2014.

[22] A. Alkhateeb, O. El Ayach, G. Leus, and R. W. Heath, "Channel estimation and hybrid precoding for millimeter wave cellular systems," *IEEE J. Sel. Top. Signal Process.*, vol. 8, no. 5, pp. 831–846, 2014.

[23] P. Wang, Y. Li, L. Song, and B. Vucetic, "Multi-gigabit millimeter wave wireless communications for 5G: From fixed access to cellular networks," *IEEE Commun. Mag.*, vol. 53, no. 1, pp. 168–178, 2015.

[24] S. Rangan, T. S. Rappaport, and E. Erkip, "Millimeter-wave cellular wireless networks: Potentials and challenges," *Proc. IEEE*, vol. 102, no. 3, pp. 366–385, 2014.

[25] C. Zhang *et al.*, "Compact Millimeter Wave Massive MIMO System Utilizing ESPAR," *IEEE Trans. Commun.*, 2025.

[26] K. Chen, H. Ding, Y. Zhu, Z. Yang, and B. Li, "Hybrid beamforming optimization design for millimeter-wave communications: A multi-scale convolutional neural network approach," *AEU-International J. Electron. Commun.*, p. 155913, 2025.

[27] Y. Chen, H. Shen, and C. Han, "Cross Far-and Near-Field Beam Management Technologies in Millimeter-Wave and Terahertz MIMO Systems," *arXiv Prepr. arXiv2504.18855*, 2025.

[28] K. Chen, C. Qi, J. Huang, O. A. Dobre, and G. Y. Li, "Near-Field Communications for Extremely Large-Scale MIMO: A Beamspace Perspective," *IEEE Commun. Mag.*, 2025.

[29] M. Majidzadeh, J. Kaleva, N. Tervo, H. Pennanen, A. Tölli, and M. Latva-aho, "Hybrid Beamforming for Mm-Wave massive MIMO systems with partially connected RF Architecture," *Wirel. Pers. Commun.*, vol. 136, no. 4, pp. 1947–1979, 2024.

[30] T. Sun, G. Zhu, X. Li, J. Fan, and M. Xia, "Low-complexity hybrid beamforming for multi-cell mmwave massive MIMO: A primitive Kronecker decomposition approach," *Signal Processing*, p. 110102, 2025.

Appendices (Derivation of the equations)

Appendix A:

Baseband Digital Beamforming: Proof of Equation (9)

With a uniform B (bits) quantization of the phase shifter, this feasible set might be described as follows:

$$\omega = \left\{\exp\left(\frac{2\pi b}{2^B}\right)\right\}_{b=1}^{2^B} \quad \dots (A\text{-}1)$$

Ensuring the total power restriction is the goal of C2, the second constraint in equation (8). Using the same methods as in reference [18], the hybrid beamformer's design to optimize bandwidth efficiency is equivalent to reducing the Euclidean distance between the hybrid beamformer and the ideal full-digital beamformer. Thus, the following is a statement of the optimal formula:

Problem: $\min_{W_{PB},W_{BB}} f_2(W_{PB},W_{BB})$ $\quad C^1: \ W_{PB}(i,j) \in \omega \quad \forall i,j$

$$C^2: \ \|W_{PB}W_{BB}\|_F^2 = M_{st} \quad \dots (A\text{-}2)$$

where, $\min_{W_{PB},W_{BB}} f_2(W_{PB},W_{BB}) = \min_{W_{PB},W_{BB}} \left\|W_{opt} - W_{PB}W_{BB}\right\|_F \ \|\cdot\|_F$, The first step is to decompose this matrix into the product of three matrices**. H=UΣV^H**, where **V** and **U** are unitary matrices (with orthonormal columns), $W_{opt} = V_1$, and **Σ** is a diagonal matrix with positive real components. As a result, the starting angles of the analog beamforming will be as follows when employing the technique recommended in our earlier work [18]. The issue may be reduced to the following statement,

$$\measuredangle \left\{W_{PB}\left(k,\frac{M_{RF}}{M_{at}}k\right)\right\}_{k=1}^{M_{at}} = \measuredangle \left\{W_{opt}{}^{(k,:)} \ W_{BB}{}^{\left(\frac{M_{RF}}{M_{at}}k,:\right)^H}\right\} \quad \dots (A\text{-}3)$$

Appendix B:

1. Baseband Digital Beamforming:

Problem (A-2) will mostly be treated as a matrix-factorizing work with two matrices parameters, W_{PB} and W_{BB}, using Alternating Minimization as the main primary technique. If the passband beamform needs to be fixed, the process is made simpler as follows:

Problem: $\min_{W_{BB}} f_3(W_{PB},W_{BB})$ $\quad$ Subject to: $\|W_{PB}W_{BB}\|_F^2 = M_{st} \quad \dots (B\text{-}1)$

where $\min_{W_{BB}} f_3(W_{PB},W_{BB}) = \min_{W_{BB}} \left\|W_{opt} - W_{PB}W_{BB}\right\|_F^2$. This work is a nonconvex quadratic problem with a quadratic constraint [23]. $\left\|W_{opt} - W_{PB}W_{BB}\right\|_F^2 = \left(W_{opt} - W_{PB}W_{BB}\right)^T \left(W_{opt} - W_{PB}W_{BB}\right)$

For minimum value, $\frac{\partial}{\partial W_{BB}}\left(W_{opt}{}^T W_{opt} - 2W_{BB}{}^T W_{PB}{}^T W_{opt} + W_{BB}{}^T W_{PB}{}^T W_{PB} W_{BB}\right) = 0$

$$W_{BB} = (W_{PB}{}^T W_{PB})^{-1} W_{PB}{}^T W_{opt} = W_{PB}{}^{\dagger} W_{opt} \quad \dots (B\text{-}2)$$

2. Passband Analog Beamforming (Riemannian-manifold)

In the next alternating phase, we solve $W_{BB}$and search for an analog beamformer that maximizes the following issue.

Problem: $\min_{W_{PB}} f_4(W_{PB},W_{BB})$,Subject to: $\|W_{PB}W_{BB}\|_F^2 = M_{st}$, $\left|(W_{PB})_{ij}\right| = 1 \ \forall$ i and j $\dots (B\text{-}3)$

$\min_{W_{PB}} f_4(W_{PB},W_{BB}) = \min_{W_{PB}} \left\|W_{opt} - W_{PB}W_{BB}\right\|_F^2$. The following is an expression for the Euclidean gradient:

$$\nabla f_4(W_{PB}) = \frac{\partial}{\partial W_{PB}}\left(W_{opt}{}^T W_{opt} - 2W_{BB}{}^T W_{PB}{}^T W_{opt} + W_{BB}{}^T W_{PB}{}^T W_{PB} W_{BB}\right)$$

$$= \text{vect}\left(-2\left(W_{opt} - W_{PB}W_{BB}\right)W_{BB}{}^H \right) \quad \dots . \ (B\text{-}4)$$

The Riemannian-gradient vector in this situation is provided as follows:

$\text{grad}\, f_4(W_{PB}) = -\text{Proj}_{W_{PB}} \nabla f_4(W_{PB}) = \nabla f_4(W_{PB}) - \text{Rel.}\left(\nabla f_4(W_{PB}).\ W_{PB}{}^*\right).\ W_{PB}$ $\dots .$ (B-5)The tangential vector α η retraction at point $w^{(t+1)}$ may be expressed in the following way:

$$w^{(t+1)} = \text{Ret}_w\left(\alpha\, \eta^{(t)}\right) = \text{vect}\left[\frac{\left(w^{(t)} + \alpha\, \eta^{(t)}\right)_i}{\left|\left(w^{(t)} + \alpha\, \eta^{(t)}\right)_i\right|}\right] \quad \dots \dots (B\text{-}6)$$